



# Radio-biologically motivated modeling of radiation risks of mortality from ischemic heart diseases in the Canadian fluoroscopy cohort study

Helmut Schöllnberger<sup>1,2</sup> · Jan Christian Kaiser<sup>1</sup> · Markus Eidemüller<sup>1</sup> · Lydia B. Zablotska<sup>3</sup>

Received: 17 November 2018 / Accepted: 24 October 2019 / Published online: 28 November 2019  
© Springer-Verlag GmbH Germany, part of Springer Nature 2019

## Abstract

Recent analyses of the Canadian fluoroscopy cohort study reported significantly increased radiation risks of mortality from ischemic heart diseases (IHD) with a linear dose–response adjusted for dose fractionation. This cohort includes 63,707 tuberculosis patients from Canada who were exposed to low-to-moderate dose fractionated X-rays in 1930s–1950s and were followed-up for death from non-cancer causes during 1950–1987. In the current analysis, we scrutinized the assumption of linearity by analyzing a series of radio-biologically motivated nonlinear dose–response models to get a better understanding of the impact of radiation damage on IHD. The models were weighted according to their quality of fit and were then mathematically superposed applying the multi-model inference (MMI) technique. Our results indicated an essentially linear dose–response relationship for IHD mortality at low and medium doses and a supra-linear relationship at higher doses (> 1.5 Gy). At 5 Gy, the estimated radiation risks were fivefold higher compared to the linear no-threshold (LNT) model. This is the largest study of patients exposed to fractionated low-to-moderate doses of radiation. Our analyses confirm previously reported significantly increased radiation risks of IHD from doses similar to those from diagnostic radiation procedures.

**Keywords** Ionizing radiation · Ischemic heart diseases · LNT model · Multi-model inference · Nonlinear dose–response

## Introduction

One of the most important questions in radiation research relates to the shape of the dose–response for different detrimental health outcomes at low exposures levels. Various international radiation protection organizations use the linear no-threshold (LNT) model to predict risks of cancer after

ionizing radiation (IR) exposures (NCRP 2018; Shore et al. 2018, 2019; ICRP 2005; UNSCEAR 2000). However, the most recent analysis of the Life Span Study (LSS) data suggests a significant quadratic upward curvature, especially for the incidence of all solid cancers in males (Grant et al. 2017). For cardiovascular diseases (CVD), doses above 5 Gy IR have been shown to be associated with a significantly elevated risk (HPA 2010). At doses between 0.5 and 5 Gy, there is clear evidence for an increased risk (HPA 2010; Kreuzer et al. 2015; Azizova et al. 2015a, 2015b; Moseeva et al. 2014). Radiation risks at low (<0.1 Gy) and low-to-moderate (0.1–0.5 Gy) doses have been examined only in a few studies with considerable discrepancies in findings and require further research (for example, Shimizu et al. 2010; Mitchel et al. 2011, 2013; Little et al. 2012; Ozasa et al. 2012, 2017; Schöllnberger et al. 2012, 2018; Simonetto et al. 2014, 2015; Takahashi et al. 2017; Gillies et al. 2017). In this context, the question whether even smallest doses of IR may increase the risk of CVD or whether nonlinear dose–response curves may be better suited to describe the health risk is of special interest. There could also be a threshold for the dose below which radiation may have no effect, or lead to either a strongly elevated risk or a

**Electronic supplementary material** The online version of this article (<https://doi.org/10.1007/s00411-019-00819-9>) contains supplementary material, which is available to authorized users.

✉ Helmut Schöllnberger  
hschoellnberger@bfs.de;  
schoellnberger@helmholtz-muenchen.de

- <sup>1</sup> Department of Radiation Sciences, Institute of Radiation Medicine, Helmholtz Zentrum München, Ingolstädter Landstrasse 1, 85764 Neuherberg, Germany
- <sup>2</sup> Division UR-Environmental Radioactivity, Federal Office for Radiation Protection, Ingolstädter Landstrasse 1, 85764 Neuherberg, Germany
- <sup>3</sup> Department of Epidemiology and Biostatistics, University of California, San Francisco, 550 16th Street, San Francisco, CA 94158, USA

protective effect. Such questions are of great importance for radiation protection, especially against the rising worldwide use of IR in medical applications. They are also relevant for occupationally exposed groups of individuals. For CVD, the question of the shape of the dose–response is as important as it is for cancer because even though relative radiation risks of CVD are smaller than radiation risks of cancer (Ozasa et al. 2012), the overall burden of disease is much larger due to high background rates of CVD in Western populations (World Health Organization 2013).

Recently, significantly elevated risks of death from ischemic heart diseases (IHD) in a cohort of tuberculosis patients from Canada exposed to low-to-moderate doses of highly fractionated X-ray radiation from repeated chest fluoroscopies were reported (Zablotska et al. 2014). The reported dose–response was strictly linear, and researchers described a novel finding of a significant inverse dose-fractionation association in IHD mortality (Zablotska et al. 2014). The aim of the present study is to investigate radiation-associated risk of IHD in the Canadian fluoroscopy cohort study (CFCS) with a larger set of radio-biologically motivated dose–response models and to comprehensively characterize model uncertainties using multi-model inference (MMI, Burnham and Anderson 2002; Claeskens and Hjort 2008; Walsh and Kaiser 2011).

## Materials and methods

### Data sources

The CFCS data have been described in detail elsewhere (Zablotska et al. 2014). The cohort includes 63,707 tuberculosis patients from Canada who were first treated for tuberculosis between 1930 and 1952 and could have received multiple fluoroscopic X-ray examinations to maintain therapeutic pneumothorax, one of the preferred treatments in the pre-antibiotic era. Most individuals in the cohort were born between 1920 and 1929 (see Table 2 in Zablotska et al. 2014). Absorbed lung doses from fluoroscopic examinations were estimated for each patient for each year since first admission for treatment of tuberculosis (Zablotska et al. 2014). For each lung dose to be estimated 100,000 simulations were carried out and an arithmetic mean of all simulations was used for dose–response analyses. The lung dose was used because it should be a reasonable surrogate for doses to the heart and associated major blood vessels (Zablotska et al. 2014). There could be substantial uncertainties in dose estimates. These are partially accounted for in the dose-estimation methods, where doses were estimated using Monte Carlo simulation techniques, which are sampled from probability distributions of various data sources and should provide a reasonable estimate of radiation doses

to the lung and heart. As stated by Zablotska et al. (2014), the impact of errors in exposure estimates in dosimetry was estimated in previous studies and shown to be relatively small and primarily of Berkson type (Howe and McLaughlin 1996) and therefore unlikely to introduce a substantial bias in risk estimates (Carroll et al. 2006).

Thirty-nine percent of the cohort (24,932 patients) were exposed to at least one fluoroscopy while the remaining 38,775 are considered unexposed to radiation from fluoroscopy. On average, exposed patients were treated 64 times with a typical fluoroscopic examination delivering a mean lung dose of 0.0125 Gy at a dose rate of approximately 0.6 mGy s<sup>-1</sup>. The mean cumulative person-year-weighted lagged lung dose among exposed was 0.79 Gy (range, 0–11.6 Gy). Doses were lagged by 10 years, a minimal latent period that has been used in several studies of long-term risks of radiation exposure on cancer and non-cancer mortality risk (Zablotska et al. 2014; Little et al. 2012; Darby et al. 2010).

Study participants had to be alive at the start of follow-up in 1950 and were followed-up for mortality until the end of 1987 with 1,902,251.68 person-years. During this time, 5818 deaths from IHD (ICD-9 codes 410–414 und 429.2) were identified through a linkage with the Canadian Mortality Database. The cohort was evenly split between men and women. Patient age at first admission for tuberculosis treatment ranged from 1 to 81 years. Additional characteristics of the CFCS are provided in Table S1 of the Online Resource.

### Statistical methods

The present analysis applied the same dataset cross-classified by sex, Canadian province of most admissions (Nova Scotia, other), type of tuberculosis diagnosis (pulmonary, nonpulmonary), stage of tuberculosis (minimal, moderate, advanced, or not specified), smoking status (unknown, non-smoker, smoker), age at first exposure (0–4, 5–9, 10–19, or 20–87 years), attained age (0–24, 25–29, ... 80–84, or 85–100 years), calendar year at risk (1950–1954, 1955–1959, ... 1980–1984, or 1985–1987), duration of fluoroscopy screenings, and 10-year cumulative lagged lung dose as (Zablotska et al. 2014). Poisson regression was based on time-dependent person-year-weighted mean cumulative dose in cross-classified cells, using excess relative risk (ERR) models in combination with a parametric baseline model.<sup>1</sup> The general form of an ERR model is

<sup>1</sup> In this study, mortality follow-up was conducted through record linkage with the Canadian Mortality Database using probabilistic linkage. The term "record linkage" refers to the process of comparing two or more records which contain identifying information to determine whether those records refer to the same individual enrolled in a cohort study. In the absence of personal identifying numbers which would allow definitive linkage to mortality outcomes (social insurance numbers were not introduced in Canada until 1964 while the

$h = h_0 \times (1 + ERR(D, Z))$ , where  $h$  is the total hazard function and  $h_0$  is the parametric baseline model.  $ERR(D, Z)$  describes the change of the hazard function with cumulative lagged lung dose  $D$  allowing for dose–effect modification by co-factor(s)  $Z$ , such as sex, age at first exposure or dose fractionation so that  $ERR(D, Z) = err(D) \times \varepsilon(Z)$ . Here,  $err(D)$  represents the dose–response and  $\varepsilon(Z)$  contains the dose–effect modifiers<sup>2</sup> (DEMs). A parametric baseline model had been developed to analyze the risk for IHD in the Mayak Workers Cohort (Simonetto et al. 2014). It was taken as guidance for developing a parametric baseline model for the CFCS data. Both models for cohorts Mayak and CFCS are provided on pages 4–6 of the Online Resource. The baseline model in equation (S4) of the Online Resource was combined with the LNT model and adjusted for dose fractionation (Zablotska et al. 2014):

$$h = h_0 \{1 + \beta_1 \times D \times \exp[\beta_2(\text{drate} - 0.2)]\}, \quad (1)$$

where  $\beta_1$  denotes the slope of the linear dose–response and  $\beta_2$  is the parameter associated with the DEM  $\text{drate} - 0.2$ . Parameter  $\text{drate}$  represents the dose fractionation, a surrogate for dose rate, defined as  $\text{drate} := D \times \text{time}^{-1}$  where  $\text{time}$  is the overall duration of fluoroscopic procedures.<sup>3</sup> The unit of  $\text{drate}$  is  $\text{Gy year}^{-1}$ . By centering  $\text{drate}$  parameter  $\beta_1$  corresponds to the risk for a patient with radiation exposures at  $0.2 \text{ Gy year}^{-1}$ , i.e., approximately 16 fluoroscopic procedures per year (Zablotska et al. 2014).

Footnote 1 (continued)

study is based on the medical records for patients first admitted for treatment during 1930–1952), study investigators used a combination of identifying items such as surname; given name; day, month, and year of birth to conduct a linkage. Each pair of linked records was assigned a probabilistic weight which depends on the likelihood of the link being true (Howe 1998). A cutoff value was then used to separate possibly true links with higher linkage weights from those less likely to be true. A higher cutoff point for the internal dose–response analysis was used to avoid dilution of any association due to the presence of false positives (i.e., false linkages); the change in cutoff would not be expected to bias estimates of relative risk. Under quite general conditions, potentially substantial bias could be introduced by using absolute risk models. Therefore, analyses with EAR models should not be performed with the CFCS data because the linkage of the cohort with the mortality registry is probabilistic which could affect absolute mortality but not relative mortality models (Zablotska et al. 2014).

<sup>2</sup> Co-factor(s)  $Z$ , such as sex, age at first exposure or dose fractionation are often referred to in radiation epidemiology as risk effect modifiers because they are factors that modulate the main central risk per unit dose estimate.

<sup>3</sup> Duration of fluoroscopic procedures, respectively, fluoroscopy screenings refers to the timespan over which fluoroscopic examinations were provided.

Subsequently, the dose–response model from Eq. (1) (i.e.,  $\beta_1 \times D$ ) was substituted by the models in Fig. 1 (Q-model–Gompertz model). They were chosen with care to reflect as many biologically plausible shapes for dose–responses as possible, including supralinear and sub-linear models. Motivations for these models from the biological scientific literature are provided in Table 1 and in the “Discussion” section. The mathematical forms and names of the functions illustrated in Fig. 1 are given in columns 1 and 2 of Table 1, respectively. Columns 3 and 4 of Table 1 state which types of radiation biological experiments have previously provided evidence for applying these functions in the present analysis, and the relevant citations of the biology papers, respectively. Mathematical details of all models in Fig. 1 are also given on page 7 of the Online Resource; that also includes the categorical model. The threshold-dose parameter ( $D_{th}$ ) contained in some models (LTH, smooth-step, sigmoid, hormesis, two-line spline) was optimized during the model fits. The smooth-step model was implemented as a modified hyperbolic tangent function, which can accommodate various different shapes. With this function, a step is not imposed a priori but results from fitting that model to data.

## Multi-model inference (MMI) method

The term MMI was coined to describe a frequentist approach to model averaging (Burnham and Anderson 2002) and has been applied to model selection in radiobiology. In contrast to Bayesian model averaging (BMA) (Hoeting et al. 1999), which is based on the evaluation of model-specific marginal likelihood functions to determine a model average, MMI relies on the Akaike Information Criterion (AIC; Akaike 1973, 1974) and AIC-based model weights for model building. BMA is computationally more demanding and only a few radiation epidemiological studies have used it to account for uncertainties in dose estimation (Little et al. 2014, 2015, Land et al. 2015, Hoffmann et al. 2017). Both BMA and MMI apply the concept of Occam’s group (Madigan and Raftery 1994, Hoeting et al. 1999, Noble et al. 2009, Kaiser and Walsh 2013), where a group of models deemed adequate for averaging is selected from a larger group of candidate models (see Fig. 1). The methods of picking models for Occam’s group can vary. For example, Walsh and Kaiser (2011) selected all published models, which have been applied to the same LSS dataset for the same endpoint, whereas Kaiser and Walsh (2013) developed a rigorous selection process based on likelihood ratio tests (LRTs).

The shape of the MMI-derived dose–response is more reliably determined than the shape for any individual dose–response because the MMI dose–response shape accounts for strengths of evidence for each of the contributing dose–response shapes. MMI also provides a more

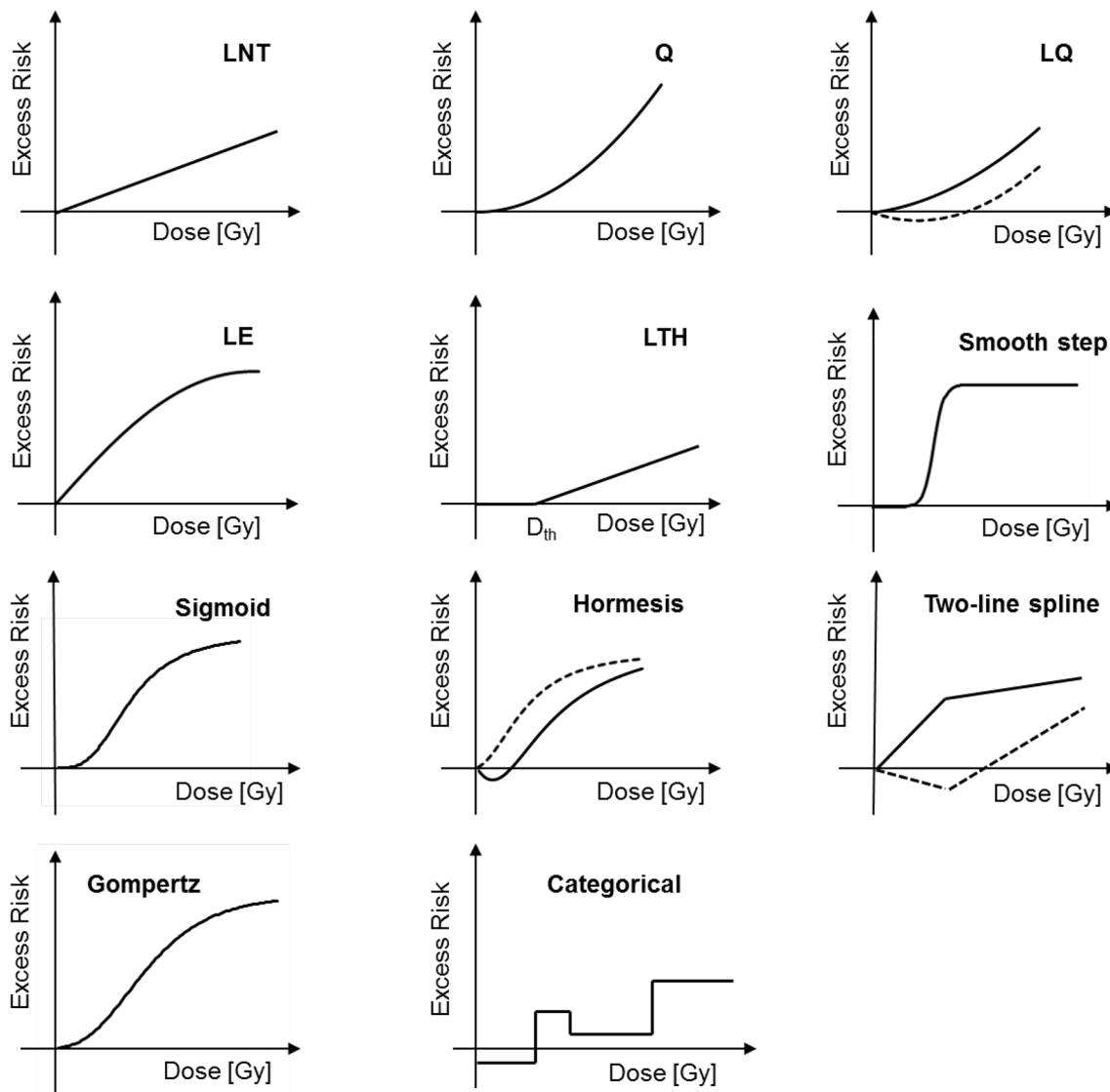


**Fig. 1** Typical shapes of the functions that were used to analyze the dose–response for IHD mortality in the Canadian Fluoroscopy Cohort Study (follow-up 1950–1987). 1st row: linear no-threshold (LNT) model, quadratic (Q), linear-quadratic (LQ); 2nd row: linear-

exponential (LE) model, linear-threshold (LTH), smooth-step model; 3rd row: sigmoid model, hormesis model, two-line spline model; 4th row: Gompertz model, categorical model. Additional dashed lines show the flexibility of some of the models

comprehensive characterization of model uncertainties by accounting for possible bias from model selection. It is a statistical method of superposing different models that all describe a certain data set about equally well (Burnham and Anderson 2002, Claeskens and Hjort 2008). In the present study, the MMI approach aims to detect nonlinearities in the dose–response by combining biologically plausible dose–responses based on goodness-of-fit.

### Model selection

To assess the influence of model-selection criteria on the risk estimates, we used two approaches. In the “sparse model

approach”, candidate dose–response models from Fig. 1 are compared using the LRT at a 95% confidence level. With this method, a small set of final non-nested models with highly significant dose–responses was identified for Occam’s group. Specifically, for each final non-nested model we calculated the AIC using the formula:

$$\text{AIC} = \text{dev} + 2 \times N_{par},$$

where dev is the final deviance and  $N_{par}$  is the number of model parameters. Models with smaller AIC are favored based on fit (via dev) and parameter parsimony (models with more parameters get punished by the factor  $2 \times N_{par}$ ) (Walsh

**Table 1** Dose–response models used for MMI and related biological studies that motivate the use of these specific models in the present study; Canadian Fluoroscopy Cohort Study, 1950-1987

$err(D)$	Name of model	Biological outcome and dose type investigated	References
$\beta_1 \times D$	LNT	Number of carotid artery lesions per animal, plaque area and inflammatory content of carotid artery lesions in ApoE <sup>-/-</sup> mice; 0 or 14 Gy of X-rays	Stewart et al. (2006)
		Number of atherosclerotic lesions in carotid arteries per animal, plaque area and plaque phenotype in ApoE <sup>-/-</sup> mice; 0, 8 Gy or 14 Gy of X-rays	Hoving et al. (2008)
$\beta_1 \times D^2$	Q	Number of atherosclerotic lesions in carotid arteries per animal, plaque area and plaque phenotype in ApoE <sup>-/-</sup> mice; 0, 8 Gy or 14 Gy of X-rays	Hoving et al. (2008) <sup>a</sup>
$\beta_1 \times D + \beta_2 \times D^2$	LQ <sup>b</sup>	See Q model	Hoving et al. (2008)
		See hormesis model	Mitchel et al. (2011)
		See hormesis model	Mitchel et al. (2013)
		See hormesis model	Ebrahimian et al. (2018)
		See LE model	Mancuso et al. (2015)
$\beta_1 \times D \times \exp(\beta_2 D)$	LE	Atherosclerotic features (plaque density, plaque size and plaque vulnerability) in ApoE <sup>-/-</sup> mice; acute irradiation with single doses of 0.3 or 6 Gy X-rays at 0.89 Gy min <sup>-1</sup> ; low-dose-rate exposures with <sup>137</sup> Cs $\gamma$ -rays (22 h day <sup>-1</sup> ) yielding cumulative total doses of 0.3 or 6 Gy in 300 days (dose rate of 1 mGy day <sup>-1</sup> or 20 mGy day <sup>-1</sup> , respectively)	Mancuso et al. (2015)
$\begin{cases} 0 & \text{for } D < D_{th} \\ \beta_1 \times (D - D_{th}) & \text{for } D \geq D_{th} \end{cases}$	LTH	Disease frequency and severity of chronic ulcerative dermatitis in <i>Trp53</i> normal ( <i>Trp53</i> <sup>+/+</sup> ) or heterozygous ( <i>Trp53</i> <sup>+/-</sup> ) female C57BL/6 mice; fractionated low-dose and low-dose-rate <sup>60</sup> Co $\gamma$ -radiation (0.33 mGy per day delivered at 0.7 mGy hr <sup>-1</sup> ; 5 days week <sup>-1</sup> ; for 30 weeks, 60 weeks or 90 weeks yielding 48 mGy, 97 mGy or 146 mGy, respectively)	Mitchel et al. (2007)
		See hormesis model	Mitchel et al. (2011)
		See hormesis model	Mitchel et al. (2013)
		See hormesis model	Ebrahimian et al. (2018)
		Inflammatory and thrombotic markers in the heart of ApoE <sup>-/-</sup> mice; total body irradiation ( <sup>60</sup> Co $\gamma$ -irradiation) with 0.025, 0.05, 0.1, 0.5 or 2 Gy at low (1 m Gy min <sup>-1</sup> ) or high dose rate (150 m Gy min <sup>-1</sup> )	Mathias et al. (2015)
		Atherosclerotic features (plaque size and phenotype, plaque inflammatory profile and oxidative stress status) in ApoE <sup>-/-</sup> mice; chronic internal exposure to <sup>137</sup> Cs via drinking water; the resulting absorbed doses were 3, 15, and 75 mGy after 6 months and 6, 30, and 150 mGy after 9 months exposure to 4, 20 and 100 kBq l <sup>-1</sup> of <sup>137</sup> Cs, respectively	Le Gallic et al. (2015)
$0.5 \times scale \times [\tanh(s(D - D_{th})) - \tanh(-sD_{th})]$	Smooth step	See LTH model	Mitchel et al. (2007)
		See LTH model	Mathias et al. (2015)
		See LTH model	Le Gallic et al. (2015)
		See hormesis model	Mitchel et al. (2011)
		See hormesis model	Mitchel et al. (2013)
		See hormesis model	Ebrahimian et al. (2018)
		See LE model	Mancuso et al. (2015)
$\lambda_0 \left( 1 - \frac{1}{1 + \left(\frac{D}{D_{th}}\right)^{\lambda_1}} \right)$	Sigmoid <sup>c</sup>	See LTH model	Mitchel et al. (2007)
		See LTH model	Mathias et al. (2015)
		See LTH model	Le Gallic et al. (2015)
		See hormesis model	Mitchel et al. (2011)
		See hormesis model	Mitchel et al. (2013)
		See hormesis model	Ebrahimian et al. (2018)
		See LE model	Mancuso et al. (2015)



**Table 1** (continued)

$err(D)$	Name of model	Biological outcome and dose type investigated	References
$\lambda_0 - \frac{\lambda_0 + \lambda_2 D}{1 + (\frac{D}{D_{th}})^{\lambda_1}}$	Hormesis <sup>d</sup>	Atherosclerotic features (aortic lesion frequency, size and severity, total serum cholesterol levels and the uptake of lesion lipids by lesion-associated macrophages) in ApoE <sup>-/-</sup> mice; 0, 0.025, 0.05, 0.10 or 0.50 Gy <sup>60</sup> Co $\gamma$ -irradiation at either low dose rate (1.0 mGy min <sup>-1</sup> ) or high dose rate (app. 0.15 Gy min <sup>-1</sup> )	Mitchel et al. (2011)
		Atherosclerotic features (aortic lesion frequency, size and severity, total serum cholesterol levels) in ApoE <sup>-/-</sup> mice with reduced <i>p53</i> function ( <i>Trp53</i> <sup>+/-</sup> ); 0, 0.025, 0.05, 0.10 or 0.50 Gy <sup>60</sup> Co $\gamma$ -irradiation at either low dose rate (1.0 mGy min <sup>-1</sup> ) or high dose rate (app. 0.15 Gy min <sup>-1</sup> )	Mitchel et al. (2013)
		Atherosclerotic development (plaque size and phenotype, inflammatory profile and oxidative stress status) in ApoE <sup>-/-</sup> mice; chronic $\gamma$ -irradiation for 8 months at 12 or 28 $\mu$ Gy hr <sup>-1</sup> , yielding cumulative doses of 67 and 157 mGy, respectively	Ebrahimian et al. (2018)
$\begin{cases} \beta_1 \times D & \text{for } D < D_{th} \\ \beta_1 \times D_{th} + \beta_2 \times (D - D_{th}) & \text{for } D \geq D_{th} \end{cases}$	Two-line spline <sup>e</sup>	See LNT model	Stewart et al. (2006)
		See LNT model	Hoving et al. (2008)
		See LTH model	Mitchel et al. (2007)
		See LTH model	Mathias et al. (2015)
		See LTH model	Le Gallic et al. (2015)
		See hormesis model	Mitchel et al. (2011)
		See hormesis model	Mitchel et al. (2013)
		See hormesis model	Ebrahimian et al. (2018)
		See LE model	Mancuso et al. (2015)
		$\begin{cases} \beta_1 \times \exp\{-\beta_2 \exp[-\beta_3 \times (D - D_{th})]\} - \\ \beta_1 \times \exp\{-\beta_2 \exp[-\beta_3 \times (-D_{th})]\} \end{cases}$	Gompertz <sup>f</sup>
See LQ model	Hoving et al. (2008)		
See LTH model	Mitchel et al. (2007)		
See LTH model	Mitchel et al. (2011)		
See LTH model	Mitchel et al. (2013)		
See LTH model	Mathias et al. (2015)		
See LTH model	Le Gallic et al. (2015)		
See LTH model	Ebrahimian et al. (2018)		
	See LE model	Mancuso et al. (2015)	

<sup>a</sup>The publication by Hoving et al. (2008) shows that female mice 30 weeks after a 14 Gy exposure exhibited a higher number of initial atherosclerotic lesions per animal compared to a linear extrapolation from the number of lesions obtained after 8 Gy (Fig. 3, panel B). Panel E of Fig. 3 in Hoving et al. (2008) shows a similar result for the mean of the individual plaque area for initial lesions in female mice 30 weeks after exposure. These findings exhibit a quadratic or linear-quadratic dose–response

<sup>b</sup>The LQ model has the capability to describe shallow U-shaped or J-shaped dose–responses (Fig. 1). Therefore, in addition to the reference Hoving et al. (2008), which gives support for the use of quadratic or linear-quadratic dose–response models, the same references are provided as for the hormesis model. In addition, the LQ model can describe supralinear dose–responses. Consequently, the reference Mancuso et al. (2015) is also listed in this context

<sup>c</sup>The sigmoid model can exhibit similar shapes as the smooth-step model. Therefore, the same references are relevant as for the smooth-step model

<sup>d</sup>This empirical hormesis model has been introduced by Brain and Cousens (1989) to describe stimulation of plant growth after low-dose herbicide exposures. Some adaptations to the model by Brain and Cousens (1989) have been made by Cedergreen et al. (2005) and Simonetto et al. (2014) to yield the specific mathematical form applied in the present study

<sup>e</sup> The two-line spline model was applied because of its capability to describe supralinear or sublinear dose–responses (Fig. 1). Therefore, the same references are provided as for the LE, LTH and hormesis models. Because it can also describe LNT dose–responses, the references Stewart et al. (2006) and Hoving et al. (2008) were added

<sup>f</sup> The Gompertz model is very flexible and can exhibit linear no-threshold dose–responses, sublinear and smooth-step responses but also supralinear dose–responses. Therefore, its use in the present study is motivated by the same biological findings referenced in the context of the LNT model, the linear-quadratic, LTH, smooth-step and linear-exponential models

**Table 2** Maximum likelihood estimates of model parameters, related 95% confidence intervals and final deviances of fitting ERR-LNT models to the mortality data for ischemic heart diseases (Zablotska et al. 2014); Canadian Fluoroscopy Cohort Study, 1950-1987

Parameter	Zablotska et al. (2014), LNT model without dose-fractionation adjustment <sup>a</sup>	Zablotska et al. (2014), LNT model with dose-fractionation adjustment <sup>a</sup>	Present study, LNT model without dose-fractionation adjustment <sup>a,b</sup>	Present study, LNT model with dose-fractionation adjustment <sup>a,c,d</sup>
$\beta_1$	0.007 Gy <sup>-1</sup> (-0.044, 0.072)	0.176 Gy <sup>-1</sup> (0.011, 0.39)	-0.046 Gy <sup>-1</sup> (-0.075, -0.013)	0.182 Gy <sup>-1</sup> (0.049, 0.33)
$\beta_2$		-10.2 years Gy <sup>-1</sup> (-25, -2.1)		-12.0 years Gy <sup>-1</sup> (-21, -5.1)
dev	9884.50	9879.76	13250.95	13247.75

dev: final deviance, ERR-LNT: linear no-threshold model implemented as excess relative risk model

<sup>a</sup>The difference between the model applied by Zablotska et al. (2014) and the one from the present study is the baseline model (stratified in the first case, parametric in the present study)

<sup>b</sup>Fit was performed with model given in Eq. (1) with  $\beta_2=0$

<sup>c</sup>Fit was performed with model given in Eq. (1)

<sup>d</sup>As a comparison, the fit of the parametric baseline model alone with its 21 parameters led to dev = 13252.68

2007). For a set of final non-nested models, AIC-weights are calculated; models with smaller AIC are assigned a larger weight (see page 9 of the Online Resource). The resulting weights, multiplied by a factor of  $10^4$ , gave a number of samples for risk estimates to be generated by uncertainty distribution simulations. We then combined model-specific probability density functions into one dataset. The resulting probability density distribution represents all uncertainties arising from the different models and their superposition. Central risk estimates from MMI were calculated from AIC-weighted maximum likelihood estimates (MLE) for single risk models. 95% confidence intervals (CI) were derived from the final merged MMI probability density distributions.

In the second, “rich model approach”, an LRT-based reduction of dose–response parameters of the candidate models was not performed. The AIC was calculated for each different model fit together with the AIC-weights. Models with bilateral AIC-weights smaller than 5% did not survive the selection process; all others were included into the set of final non-nested models. This approach leads to a larger number of models deemed suitable for MMI. The calculation of AIC-weights for the two sets (or Occam’s groups) of dose–response models based on both approaches (“sparse” versus “rich”) is detailed on page 9 of the Online Resource. The software used to perform all analyses is briefly introduced on page 10 of the Online Resource.

## Results

Similar to the previously published results (Zablotska et al. 2014), the slope parameter  $\beta_1$  was not significant without adjustment for dose fractionation ( $\beta_1 = -0.046$  Gy<sup>-1</sup>, Table 2). Adjustment led to a significant *ERR* per dose = 0.182 Gy<sup>-1</sup> with 95% CI (0.049, 0.325) (Table 2) (*ERR* per dose = 0.176 Gy<sup>-1</sup> in Zablotska et al. 2014).

Subsequently, the LNT model from Eq. (1) was substituted by all other models from Fig. 1, keeping the DEM *drate* = 0.2.

Considering the relations in Figure S1 of the Online Resource and a sparse model approach, four final non-nested models survived the selection process and were included into Occam’s group: LNT, Q, two-line spline<sup>4</sup> and the Gompertz models. For these four models, the model parameters (baseline and radiation-associated), their MLE and symmetric, Wald-type standard errors are provided in Table S2 of the Online Resource. Details related to model selection according to the sparse model approach are provided in the Online Resource (see pages 9, 15, 16, and Table S3).

According to the rich model approach, 10 models survived the selection process and contributed to MMI with normalized weights provided in Table 3. Figure 2 shows the *ERR* plotted against the cumulative lagged lung dose for the four final non-nested models and for the simulated dose–response curve from MMI, calculated with the sparse and the rich model approaches. Figures 3 and 4 show the best models and MMI for doses < 2 and 0.1 Gy, respectively. Table 4 provides risk predictions based on MMI (sparse) and the LNT, Q, two-line spline and Gompertz models. The radiation-associated excess cases according to the four final non-nested models and MMI (sparse) are presented in Table 5.

The Gompertz model had the best fit to the data (Table 3). Both Q and Gompertz models predicted no increase in risk below 0.05 Gy (Fig. 4). While both models predicted

<sup>4</sup> It is noted that the two-line spline model is nested with the LNT model. This can be seen in Figure S1 of the Online Resource: The two-line spline model is nested with the LTH model and the latter is nested with the LNT model (in general, Model A is nested in Model B if the parameters in Model A are a subset of the parameters in Model B). The reason why the two-line spline model was nonetheless included into Occam’s group is explained on pages 15 and 16 of the Online Resource.

**Table 3** Results of fitting the dose–response models from Fig. 1 as ERR models to the mortality data for ischemic heart diseases (Zablotska et al. 2014); Canadian Fluoroscopy Cohort Study, 1950–1987

	dev <sup>a</sup>	$\Delta$ dev <sup>b</sup>	$N_{par}$	AIC <sup>c</sup>	$\Delta$ AIC <sup>d</sup>	Normalized AIC-weights, sparse model approach <sup>e</sup>	Normalized AIC-weights, rich model approach <sup>f</sup>
ERR-LNT	13247.75	6.19	23	13293.75	2.19	0.1183	0.0776
ERR-Q	13246.01	4.46	23	13292.01	0.46	0.2815	0.1847
ERR-LQ	13245.38	3.83	24	13293.38	1.83		0.0930
ERR-LE	13245.68	4.13	24	13293.68	2.13		0.0802
ERR-LTH, $D_{th}=0.58$ Gy	13246.81	5.26	24	13294.81	3.26		0.0455
ERR-smooth-step, $D_{th}=4.47$ Gy	13244.45	2.90	25	13294.45	2.90		0.0546
ERR-sigmoid, $D_{th}=41.53$ Gy	13245.94	4.39	25	13295.94	4.39		0.0259
ERR-hormesis, $D_{th}=3.28$ Gy	13242.84	1.29	26	13294.84	3.29		0.0449
ERR-two-line spline, $D_{th}=1.72$ Gy	13242.28	0.73	25	13292.28	0.73	0.2461	0.1615
ERR-Gompertz, $D_{th}=0$	13241.55	0	25	13291.55	0	0.3541	0.2323
ERR-categorical	13242.19	0.63	29	13300.19	8.63		

AIC: Akaike Information Criterion, dev: final deviance, ERR-LNT: linear no-threshold model implemented as excess relative risk model, ERR-Q: quadratic model implemented as excess relative risk model, ERR-LQ: linear-quadratic model implemented as excess relative risk model, ERR-LE: linear-exponential model implemented as excess relative risk model, ERR-LTH: linear-threshold model implemented as excess relative risk model

<sup>a</sup>As a comparison, the fit of the baseline model alone with its 21 parameters led to dev = 13252.68

<sup>b</sup>The difference in final deviance is denoted by  $\Delta$ dev with respect to the model with the smallest final deviance

<sup>c</sup>AIC = dev +  $2 \times N_{par}$ , where  $N_{par}$  is the number of model parameters

<sup>d</sup>The difference in AIC-values with respect to the model with the smallest AIC-values is denoted by  $\Delta$ AIC

<sup>e</sup>According to the sparse model approach four models survive the selection process and are used for MMI. The normalized AIC-weights provided here were calculated with equation (S5) of the Online Resource

<sup>f</sup>According to the rich model approach all models except the categorical model survive the selection process because when compared to the model with  $\Delta$ AIC = 0 they have an AIC-weight > 0.05 (see Table S3 of the Online Resource). The normalized AIC-weights provided here were calculated with equation (S5) of the Online Resource

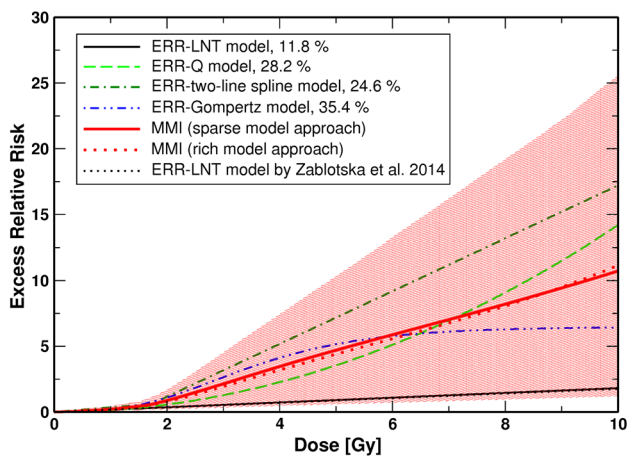
a sublinear dose–response at low and medium doses up to ~ 1 Gy, the two-line spline model predicted a risk higher than all other models (Figs. 2 and 3). The ERR predictions from MMI and LNT model at 0.1 Gy and 1 Gy are identical within their 95% CI (Table 4) and the dose–response from MMI is roughly linear at low doses (Fig. 4). At low and medium doses up to ~ 1 Gy, MMI and the LNT model predict similar risk values (Fig. 3). Consequently, up to 1 Gy both models (LNT and MMI) predict very similar excess cases (Table 5). At doses > 1.5 Gy, the dose–response from MMI predicted a higher risk compared to the LNT model (Figs. 2 and 3, Table 4). For the entire dose range, the dose–responses from MMI calculated using both the sparse and the rich model approaches were similar to each other (Figs. 2 to 4). For example, at 1 Gy, MMI predicted an ERR of 0.216 with 95% CI (0.062, 0.48) and ERR = 0.218 with 95% CI (0.058, 0.473), for rich and sparse model approaches, respectively.

Figure S2 of the Online Resource shows the baseline cases as predicted by the ERR-LNT model versus attained age with the secular trend together with crude rates.

## Discussion

CFCS is the largest cohort of patients exposed to fractionated low-to-moderate doses of IR via fluoroscopic X-rays. About 15.5% of exposed CFCS patients were exposed to doses < 0.1 Gy and thus provide direct evidence of possible risks from low-dose exposures such as CT scans (like fluoroscopic examinations, CT scans in their most commonly known form apply X-rays). We examined ten biologically plausible dose–response models together with a categorical model. At low and medium doses the MMI technique predicted an almost linear dose–response.





**Fig. 2** ERR for IHD mortality in the Canadian Fluoroscopy Cohort Study (follow-up 1950–1987) versus cumulative lagged lung dose for the four final non-nested ERR models (Table 3) and the simulated dose–response curves from MMI, calculated with the sparse model approach and the rich model approach. The shaded area represents the 95% CI region for the MMI (sparse model approach). For AIC-weights see the insert. The dotted-straight line shows the risk prediction from (Zablotska et al. 2014). The ERR-LNT model from the present study and the LNT model from Zablotska et al. (2014) give almost identical risk predictions. The figure is valid for males and females. A dose fractionation of 0.2 Gy year<sup>-1</sup> was assumed. Point estimates and related 95% CI from the fit of an ERR-categorical model that divides the dose range into the following categories ( $D < 10^{-6}$  Gy,  $10^{-6}$  Gy  $\leq D < 1$  Gy, 1 Gy  $\leq D < 2$  Gy, 2 Gy  $\leq D < 6$  Gy, and  $D \geq 6$  Gy) are as follows:  $ERR = 0.0089$  (−0.0173, 0.0348),  $ERR = 0.1820$  (−0.0652, 0.428),  $ERR = 1.002$  (−0.225, 2.23),  $ERR = 10.3$  (−17.8, 38.1). In the categorical fit, zero risk was assigned to the dose range  $D < 10^{-6}$  Gy. The point estimates and their 95% CI are not shown in the figure because of the very large 95% CI for the highest dose category. Online version contains color

While the sparse model selection approach led to a set of four final non-nested models, the rich model approach yielded an Occam’s group that contained ten out of the eleven dose–response models that were fitted to the data. Both sets of dose–response models describe the data approximately equally well (see values of  $\Delta AIC$  in Table 3).

The reason for MMI-predicted risks being significantly higher compared to the LNT model at doses  $> 1.5$  Gy is the relatively strong contributions of the Q, two-line spline and Gompertz models to the MMI (88% of the total, Table 3). At 5 Gy, MMI predicted an approximately fivefold risk compared to the LNT model, at 10 Gy a sixfold risk.

To better understand predicted radiation risks at higher doses, we used a restriction analysis based on cohort data with restricted dose-ranges and observed that the second slope of the two-line spline model ( $\beta_2$ ) was driven by high doses ( $> 2$  Gy). When restricting the data to doses smaller than 2 Gy, the first slope ( $\beta_1$ ) of this model became very similar to the slope of the LNT model (results not shown).

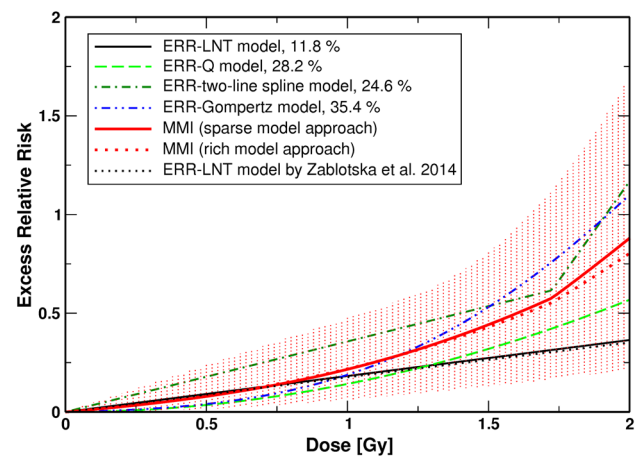


**Fig. 3** ERR for IHD mortality in the Canadian Fluoroscopy Cohort Study (follow-up 1950–1987) versus cumulative lagged lung dose up to 2 Gy for the four final non-nested ERR models (Table 3) and the simulated dose–response curves from MMI, calculated with the sparse model approach and the rich model approach. Vertical-dotted lines represent the 95% CI region for the MMI (sparse model approach). For AIC-weights see the insert. The dotted-straight line shows the risk prediction from (Zablotska et al. 2014). The figure is valid for males and females. A dose fractionation of 0.2 Gy year<sup>-1</sup> was assumed. Online version contains color

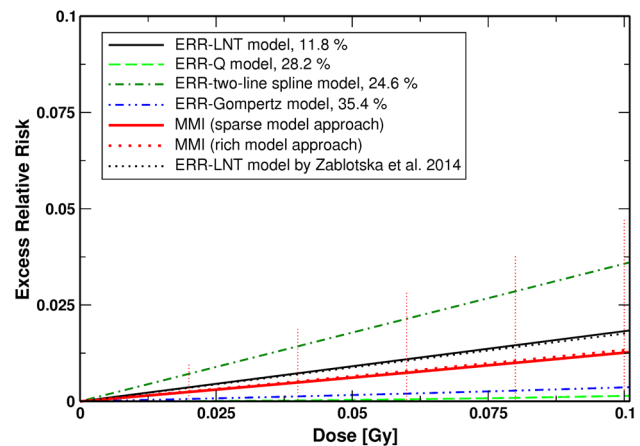


**Fig. 4** ERR for IHD mortality in the Canadian Fluoroscopy Cohort Study (follow-up 1950–1987) versus cumulative lagged lung dose up to 0.1 Gy for the four final non-nested ERR models (Table 3) and the simulated dose–response curves from MMI, calculated with the sparse model approach and the rich model approach. Vertical-dotted lines represent the 95% CI region for the MMI (sparse model approach). For AIC-weights see the insert. The dotted-straight line shows the risk prediction from (Zablotska et al. 2014). The figure is valid for males and females. A dose fractionation of 0.2 Gy year<sup>-1</sup> was assumed. Online version contains color

The LNT model was influenced mostly by doses  $< 2$  Gy. The higher doses hardly influence the slope of the LNT model due to the lower number of cases in this dose range

**Table 4** Values for *ERR* for mortality from ischemic heart diseases (Zablotska et al. 2014) at various cumulative lung doses calculated with MMI (sparse model approach) and the four final non-nested models; Canadian Fluoroscopy Cohort Study, 1950–1987

Lung dose (Gy)	MMI <sup>a,b</sup>	ERR-LNT model <sup>b,c</sup>	ERR-Q model <sup>b</sup>	ERR-two-line spline <sup>b</sup>	ERR-Gompertz <sup>b</sup>
0.1	0.01263 (0.00075, 0.048)	0.0182 (0.0045, 0.032)	0.0014 (0.00049, 0.0024)	0.036 (0.017, 0.054)	0.0036 (0.0013, 0.0060)
0.2	0.0266 (0.0028, 0.095)	0.0364 (0.0089, 0.064)	0.0057 (0.0020, 0.0094)	0.071 (0.035, 0.11)	0.0089 (0.0033, 0.015)
0.5	0.079 (0.016, 0.24)	0.091 (0.022, 0.16)	0.036 (0.012, 0.059)	0.179 (0.087, 0.27)	0.040 (0.015, 0.066)
1	0.216 (0.062, 0.48)	0.182 (0.045, 0.32)	0.142 (0.049, 0.24)	0.36 (0.17, 0.54)	0.188 (0.070, 0.31)
2	0.88 (0.21, 1.7)	0.364 (0.089, 0.64)	0.57 (0.20, 0.94)	1.17 (0.64, 1.7)	1.1 (0.41, 1.8)
5	4.70 (0.60, 10)	0.91 (0.22, 1.6)	3.6 (1.2, 5.9)	7.2 (2.3, 12)	5.2 (1.9, 8.5)
10	11 (1.2, 26)	1.82 (0.45, 3.2)	14.2 (4.9, 24)	17.2 (4.8, 30)	6.4 (2.4, 11)

ERR-LNT: linear no-threshold model implemented as excess relative risk model, ERR-Q: quadratic model implemented as excess relative risk model, MMI: multi-model inference

<sup>a</sup>Calculated with the sparse model approach

<sup>b</sup>95% CI are provided in parenthesis

<sup>c</sup>As a comparison, the *ERR* per dose from Zablotska et al. (2014) is 0.176 Gy<sup>-1</sup> with 95% CI (0.011, 0.393)

**Table 5** Radiation-associated excess cases for the mortality data for ischemic heart diseases (Zablotska et al. 2014) according to the four final non-nested models and MMI (sparse model approach); Canadian Fluoroscopy Cohort Study, 1950–1987

Dose-bin (Gy)	MMI <sup>a</sup>	ERR-LNT	ERR-Q	ERR-two-line spline	ERR-Gompertz
0–0.05	2.8	5.7	0.2	7.4	0.6
0.05–0.1	1.1	2	0.2	2.7	0.3
0.1–0.2	1.3	2.2	0.3	3.3	0.3
0.2–0.3	2.8	4	0.8	7.5	0.7
0.3–0.4	2.6	3.8	1.1	6.4	0.7
0.4–0.5	3.6	4.8	1.8	8.4	1.4
0.5–0.75	8.9	10	4.6	20.2	4
0.75–1	11.5	11.7	7.2	23.1	6.9
1–1.5	19.7	15.6	12.3	33.9	17
1.5–2	14	8.9	9.4	19.9	15.2
2–3	18	6.2	8.2	32.6	19.7
3–4	7.8	2	3.8	13.3	9.1
4–5	3.3	0.7	1.7	5.4	3.9
5	4.7	1.1	3.6	7.3	5
Sum	102.1	78.7	55.2	191.4	84.8

ERR-LNT: linear no-threshold model implemented as excess relative risk model, ERR-Q: quadratic model implemented as excess relative risk model, MMI: multi-model inference

<sup>a</sup>Calculated with the sparse model approach

(212 cases out of 5818). Thus, the fit of the two-line spline model, which predicts a more than two times higher number of excess cases than the LNT model (Table 5), is consistent with the fit of the latter model.

The present study applied a larger range of biologically realistic smooth dose–response models (Fig. 1). Exploring a larger range of different dose–response models is motivated

by the following biological findings, which are summarized in Table 1. The use of the LNT model finds support from the study of Stewart et al. (2006). These researchers investigated the effects of a high-dose (14 Gy) exposure on the development of atherosclerotic plaques (number of lesions, plaque area and plaque composition) in ApoE<sup>-/-</sup> mice. They found that after the high-dose exposure the mean number of atherosclerotic lesions (initial plus advanced) in carotid arteries of irradiated mice was significantly larger than in age- and sex-matched controls. Their study also revealed a significantly enhanced inflammatory content and plaque hemorrhage of irradiated carotid artery lesions compared to controls (Stewart et al. 2006). Because only one high-dose exposure was investigated, these findings infer an LNT-like dose–response. Analyses with a quadratic or linear-quadratic model are supported by the work of Hoving et al. (2008). They found that the number of initial atherosclerotic lesions and the plaque area in female mice 30 weeks after exposure to 0, 8 or 14 Gy clearly exhibit a dose–response consistent with a quadratic or linear-quadratic response (see panels B and E in their Fig. 3). In addition, some of the findings reported by Hoving et al. (2008) support the use of an LNT model. The specific feature of the linear-quadratic model that it can exhibit a U-shape at low doses is supported by the findings of Mitchel et al. (2011, 2013) and Ebrahimiian et al. (2018). The findings of these three studies will be briefly described below in the context of the hormesis model. The application of the linear-exponential model is justified because of the findings by Mancuso et al. (2015) related to atherogenesis in ApoE<sup>-/-</sup> mice. Although the pattern of radiation-induced aortic alterations and their severity increased at 6 Gy compared with a 20-fold lower dose of 0.3 Gy, their results tend to be far from linearity and suggest that lower doses may be more damaging than predicted by a

linear dose–response (Mancuso et al. 2015). The LTH model is another realistic possibility for a dose–response related to radio-epidemiological cohorts given the findings from animal studies on protective anti-inflammatory effects induced by low doses of radiation (Mitchel et al. 2011, 2013; Mathias et al. 2015; Le Gallic et al. 2015; Ebrahimian et al. 2018). Investigating the expression of various inflammatory and thrombotic markers in the heart of ApoE<sup>-/-</sup> mice, Mathias et al. (2015) provided evidence for anti-inflammatory effects after 0.025–0.5 Gy exposures: they found slight decreases of ICAM-1 levels and reduction of Thy 1 expression at these doses. In contrast, an enhancement of MCP-1, TNF $\alpha$  and fibrinogen at 0.05–2 Gy indicated a proinflammatory and prothrombotic systemic response (Mathias et al. 2015). In such a situation, a LTH model may describe the data better than the LNT model. Interestingly, Mitchel et al. (2007) reported that their dermatitis data from C57BL/6 J mice indicate that low doses may generally produce either no effect or protective effects with respect to this autoimmune-type and age-related non-cancer disease that has been linked to inflammation (Williams et al. 2012). The findings of anti-inflammatory protective effects at low doses (Mitchel et al. 2007, 2011, 2013, Mathias et al. 2015, Le Gallic et al. 2015, Ebrahimian et al. 2018) and detrimental effects at moderate (0.3 Gy) and higher doses (6 Gy) (Mancuso et al. 2015) provide a biological context for applying the smooth-step model (Fig. 1). A step-type response (with a steep slope) may reflect the distinct dose at which protective mechanisms are lost. Different tissues and different individuals can be expected to have different threshold-doses, leading to an overall smooth transition. While at low doses it is feasible that risk increase may be balanced by a protective decrease as in the LTH model, a smooth transition zone may exist where risk increases steadily, followed by a plateau. The sigmoid model can exhibit similar shapes as the smooth-step model. Therefore, the same references are relevant as for the smooth-step model (Mitchel et al. 2007, 2011, 2013; Mathias et al. 2015; Le Gallic et al. 2015; Mancuso et al. 2015; Ebrahimian et al. 2018). The empirical hormesis model applied in the current study has been introduced to describe stimulation of plant growth after low-dose herbicide exposures (Brain and Cousens 1989). Dose–responses which allow for protective effects at low doses, such as LQ, hormesis and two-line spline models, can be justified from mouse studies (Mitchel et al. 2011, 2013). Mitchel et al. (2011) exposed ApoE<sup>-/-</sup> mice to 0.025, 0.05, 0.10 or 0.50 Gy <sup>60</sup>Co  $\gamma$ -irradiation at either low dose rate (1.0 mGy min<sup>-1</sup>) or high dose rate (approximately 0.15 Gy min<sup>-1</sup>) and investigated biological endpoints associated with atherosclerosis (aortic lesion frequency, size and severity, total serum cholesterol levels and the uptake of lesion lipids by lesion-associated macrophages). In general, low doses given at low dose rate during either early- or late-stage disease were

protective, slowing the progression of the disease by one or more of these measures (Mitchel et al. 2011). The influence of low doses (0.025, 0.05, 0.10 or 0.50 Gy) of <sup>60</sup>Co  $\gamma$ -irradiation at low dose rate (1.0 mGy min<sup>-1</sup>) or high dose rate (approximately 0.15 Gy min<sup>-1</sup>) on atherosclerosis in ApoE<sup>-/-</sup> mice with reduced *p53* function was investigated by Mitchel et al. (2013). Radiation exposure to doses as low as 25 mGy at early-stage disease, at either the high or the low dose rate, inhibited lesion growth, decreased lesion frequency and slowed the progression of lesion severity in the aortic root. In contrast, exposure at late-stage disease produced generally detrimental effects. Both low- and high-dose-rate exposures accelerated lesion growth and high-dose-rate exposures also increased serum cholesterol levels. All effects were highly nonlinear with dose (Mitchel et al. 2013). An increase in anti-inflammatory and anti-oxidative parameters resulting in atherosclerotic plaque size reduction in ApoE<sup>-/-</sup> mice after chronic exposure to external low-dose  $\gamma$ -radiation was reported by Ebrahimian et al. (2018). Their results suggest that chronic low-dose gamma irradiation induces an upregulation of organism defenses leading to a decrease in inflammation and plaque size. Low-dose induced anti-inflammatory effects which play an important role in that context are currently intensely studied (see for example the reviews by Rödel et al. 2012a, 2012b, Frey et al. 2015) and have also been reported by Le Gallic et al. (2015) and Mathias et al. (2015). Earlier, low doses of  $\gamma$ -radiation delivered at low dose rates exhibited a protective effect related to chronic ulcerative dermatitis, an inflammatory skin reaction, in C57BL/6 mice, decreasing both disease frequency and severity and extending the lifespan of older animals (Mitchel et al. 2007). The two-line spline model can describe supra-linear or sublinear dose–responses (Fig. 1) but also linear dependencies. Therefore, its application in the present study finds support from the same studies referenced in the context of the LNT model, the linear-exponential, LTH and hormesis models (refer to Table 1). The Gompertz model can exhibit linear, sublinear and smooth-step dose–responses but also supralinear responses. Therefore, its use in the present study is motivated by the same biological findings referenced in the context of the LNT model, the linear-quadratic, LTH, smooth-step and linear-exponential models, see Table 1.

Interpretation of our findings is limited by the absence of information on important independent risk factors for CVD in the CFCS data (Zablotska et al. 2014), particularly socioeconomic status and smoking. Only a limited amount of information is available on smoking for approximately 20% of the cohort (smoking was therefore not included in the baseline model, in accordance with Zablotska et al. 2014). Some studies suggest that these factors account for a substantial proportion of observed increase in CVD (see for example Yusuf et al. 2004). However, smoking was not associated with radiation (Zablotska et al. 2014), so could not be

considered as a confounding variable in the current analyses. Furthermore, numerous recent studies found weak evidence for interaction between radiation and smoking (for example, Kreuzer et al. 2018). The CFCS data also lack information on other important CVD risk factors, such as family history of heart disease, diabetes, high blood pressure, obesity, and cholesterol plasma levels. However, because these factors are unlikely to be associated with radiation dose, they are unlikely to have biased the observed association between exposure and IHD mortality (Zablotska et al. 2014).

Another limitation is that all study participants had tuberculosis. We are aware that the precise relationship of radiation dose to IHD risk in immunocompromised, chronically ill tuberculosis patients may well differ from that in healthy individuals.

Our study findings are also limited by the end of follow-up in 1987 (Zablotska et al. 2014). It is noted that out of the 63,707 tuberculosis patients 34,717 individuals were still alive at the end of follow-up. CFCS study investigators are in the process of extending mortality follow-up by 30 years (1988–2017). In addition, they will also conduct, for the first time, cancer incidence follow-up of the cohort during 1969–2017. New doses to all organs within and outside the field of fluoroscopic irradiation will be estimated using computerized phantoms specific to the CFCS population.

Within the approach of the present study, the dose fractionation proportionally affects the magnitude of the dose–response function but not the shape of the dose–response. Given evidence of a significant inverse dose–fractionation association in the primary analysis (Zablotska et al. 2014), it seems to be a hypothesis of interest that the dose–response shape might differ by the dose rate, i.e., dose fractionation (while the person-year-weighted mean dose fractionation within the whole cohort is  $0.109 \text{ Gy year}^{-1}$ , for mean cumulative person-year-weighted lagged lung doses  $\leq 0.1 \text{ Gy}$  and  $> 0.1 \text{ Gy}$  that quantity is  $0.008 \text{ Gy year}^{-1}$  and  $0.101 \text{ Gy year}^{-1}$ , respectively). To investigate whether there may be any difference in the shape of the dose–responses at low- and high-dose fractionations the analyses of the present study could in principle be repeated within several strata of dose rate. Zablotska et al. (2014) performed such an analysis and calculated the *ERR* for three categories of dose fractionation. For IHD an inverse dose–fractionation association was found using the LNT dose–response model (see Table 6 in the publication by Zablotska et al. 2014). While such an effort is beyond the scope of the present study, there is also concern that such an in-depth analysis performed in the context of MMI may outstrip the CFCS data in terms of their ability to characterize risk of subsequent IHD in meaningful populations due to the above mentioned absence of information on classical modifiable cardiovascular risk factors such as lipids, hypertension, diabetes, abdominal obesity, diet, psychosocial factors, etc., as well as family history of IHD.

Generally, inference based on a set of multiple plausible models is a sound alternative to inference relying only on a single “best” model when the uncertainty in the model selection is large. The pitfall of using the MMI approach is, however, related to that specific aspect: the subjectivity of the model selection. In the present study, this problem is addressed with a two-tiered strategy. On the one hand, as already stated above, the models in Fig. 1 are carefully chosen to reflect as many biologically plausible shapes for dose–responses as possible. On the other hand MMI was applied in two different approaches, sparse and rich, as described in the “Materials and methods”. In the center of the case-weighted means (case-weighted mean age, case-weighted mean dose, etc.) all models yield similar risks. Only at the borders of the data space where only a few cases are located the calculated risks will differ strongly. Here, MMI helps with the comprehensive characterization of uncertainties.

In the context of subjectivity of model selection the following aspect is noted. It would be generally possible to choose a larger number of non-nested plausible models (of the same or similar number of parameters) that could lead to fits of similar shapes. That way one could end up with a situation of having a very large number of models in the set of final non-nested models, each of which with a very small AIC-weight. This situation is prevented by only including into Occam’s group those non-nested models with a bilateral AIC-weight larger than 5% (see Table S3 of the Online Resource including the related footnote e).

At low and medium doses our results are in agreement with the earlier findings (Zablotska et al. 2014) and based on a more comprehensive analysis with a larger series of biologically plausible dose–responses. An essential difference with the primary analysis (Zablotska et al. 2014) is the use of a different baseline model. The present study applied the parametric baseline model given in equation (S4) of the Online Resource with 21 baseline parameters while in (Zablotska et al. 2014) a stratified baseline model with one free parameter for each possible combination of available categories in the data was used. Their baseline model contained several thousand free parameters and was not suitable for AIC-based MMI analysis for which parsimony in parameters is essential (Walsh and Kaiser 2011).

In a recent MMI-based analysis of the LSS mortality data for heart diseases observed during 1950–2003 an *ERR* of 0.08 at 1 Gy with 95% CI (0, 0.20) was reported (Schöllnberger et al. 2018). Shimizu et al. (2010) reported an *ERR* per dose of  $0.14 \text{ Gy}^{-1}$  with 95% CI (0.06, 0.23). Within the error bars these values are consistent with our estimate of 0.216 at 1 Gy with 95% CI (0.062, 0.48). For IHD, however, these authors did not find a significant association between radiation exposure and IHD (refer to Web Table B in Shimizu et al. 2010). The latest analysis of the



LSS mortality data with extended follow-up from 1950 to 2008 found no significant association between radiation exposure and IHD either (Takahashi et al. 2017). For IHD mortality in male Mayak workers, an *ERR* per dose of  $0.09 \text{ Gy}^{-1}$  with 95% CI (0.02, 0.16) was reported (Simonetto et al. 2014). This value is consistent with the risk prediction from the present study. For females, no significant elevation in risk was found (Simonetto et al. 2014). Azizova et al. (2015a) did not find a significant association of total dose from external  $\gamma$ -rays with IHD mortality in Mayak workers. A population-based case–control study of major coronary events (i.e., myocardial infarction, coronary revascularization, or death from IHD) in 2168 women who underwent radiotherapy for breast cancer between 1958 and 2001 in Sweden and Denmark was conducted by Darby et al. (2013). The study included 963 women with major coronary events and 1205 controls. Rates of major coronary events increased linearly with the mean dose to the heart by 7.4% per gray (95% confidence interval, 2.9 to 14.5;  $P < 0.001$ ), with no apparent threshold (this corresponds to an *ERR* per dose of 0.074 with 95% CI (0.029, 0.145)). Darby and colleagues had applied a linear dose–response model. In that context it is noted that Schneider et al. (2017) put forward arguments that the dose–response may not necessarily be linear. It follows from Darby et al. (2013) that for a mean heart dose of 5 Gy  $ERR = 0.37$  with 95% CI (0.15, 0.73). The value of  $ERR = 0.37$  is considerably lower than our MMI estimate for 5 Gy (see Table 4:  $ERR = 4.70$  at 5 Gy with 95% CI (0.60, 10)). Ghobadi et al. (2012) report results from rodent experiments showing that irradiation of heart, lung, or both independently induces specific cardiac dysfunction and pulmonary vascular damage, mutually enhancing each other. Their findings suggest that irradiation of an already diseased lung can indirectly increase the IHD risk, compared to irradiation of a healthy lung. We may hypothesize that this biological effect increases the IHD risk significantly compared to LNT behavior at doses above 2 Gy, which are concomitantly associated with long duration of tuberculosis.

There remains considerable controversy over the effects of dose-protraction on long-term health outcomes. In fact, the ICRP is putting a major effort into evaluating the many modern studies with dose-protraction (Shore et al. 2017). Survivors of atomic bombings in Hiroshima and Nagasaki were exposed to acute exposure and could not provide useful information on the effects of dose fractionation. Limited data exist on the dose rate effects in Mayak workers, primarily in the form of annual absorbed doses. In contrast, the CFCS has detailed exposure information on the dose and dose rate of a typical fluoroscopic examination and number of fluoroscopic procedures for each patient per year. Altogether, the CFCS is the largest study of patients

exposed to moderately fractionated low-to-moderate doses of IR and presents one of the most valuable cohorts worldwide to derive information related to radiation effects at low, moderate and high doses of IR.

For IHD mortality among 308,297 nuclear industry workers from France, United Kingdom and United States, as part of the International Nuclear Workers Study (INWORKS), an *ERR* per dose of  $0.18 \text{ Sv}^{-1}$  with 90% CI (0.004, 0.36) was reported (Gillies et al. 2017). Recently, the CFCS data for IHD (Zablotska et al. 2014) were combined with a cohort of tuberculosis fluoroscopy patients from Massachusetts and analyzed with a linear dose–response model applying two different dose regimes with a fixed cut-point at 0.5 Gy (Tran et al. 2017). The authors reported increasing trends for doses  $< 0.5 \text{ Gy}$ ; over the entire dose range a negative dose trend was observed (Tran et al. 2017). This is probably due to the inability to adjust for dose fractionation effects in the Massachusetts data where only cumulative doses to the lung have been estimated. The present study used a more comprehensive and flexible approach by analyzing the data with a variety of different linear and nonlinear models including those that exhibit flexible threshold-doses without applying artificial cut-points at certain doses and without relying on LNT as a foregone conclusion (Little et al. 2012, Little 2016).

## Conclusions

The present study confirms previous findings in a number of studies of essentially linear dose–response for death from IHD at low and moderate doses (0–1 Gy). Our analyses suggest that different biological mechanisms may operate at low and medium doses compared to high doses and that at higher doses, the LNT model may underestimate the risk compared to the dose–response from MMI by a factor of 5. Our results should be of particular interest to international radiation protection organizations, which largely rely on analyses of radio-epidemiological cohorts using the LNT model. We conclude that our findings have important implications for risk assessment of IR in the context of medical applications (such as CT scans and radiotherapy), nuclear energy production and accident related long-term risks.

**Acknowledgements** This work was supported by a project from the Federal Office for Radiation Protection (BfS) (contract no. 3615S42221). The project has also received funding from the Euratom research and training program 2014–2018 under grant agreement No 755523 (MEDIRAD). Dr. Zablotska's work was supported by the National Cancer Institute of the National Institutes of Health (award numbers R03CA188614 and R01CA197422). We thank Dr. Michaela Kreuzer (BfS) for valuable comments related to a project report for BfS and for her support of the BfS project mentioned above. We would also like to thank Dr. Peter Jacob (RADRISK, D-83727 Schliersee) and



Dr. Axel Böttger at the Federal Ministry for the Environment, Nature Conservation and Nuclear Safety (BMU) and the BMU for enabling the BfS project. We are very grateful to the reviewers for taking the time to perform the reviews and for their valuable comments.

## Compliance with ethical standards

**Conflict of interest** The authors declare that they have no conflict of interest.

**Human and animal rights** This article does not contain any studies with human participants or animals performed by any of the authors.

## References

- Akaike H (1973) Information theory and an extension of the maximum likelihood principle. In: Petrov BN, Caski F (eds). In: Proceedings of the second international symposium on information theory. Akademiai Kiado, Budapest, pp 267–281
- Akaike H (1974) A new look at the statistical model identification. *IEEE Trans Autom Control* 19:716–723
- Azizova TV, Grigoryeva ES, Haylock RG, Pikulina MV, Moseeva MB (2015a) Ischaemic heart disease incidence and mortality in an extended cohort of Mayak workers first employed in 1948–1982. *Br J Radiol* 88:20150169
- Azizova TV, Grigorjeva ES, Hunter N, Pikulina MV, Moseeva MB (2015b) Risk of mortality from circulatory diseases in Mayak workers cohort following occupational radiation exposure. *J Radiol Prot* 35:517–538
- Brain P, Cousens R (1989) An equation to describe dose responses where there is stimulation of growth at low doses. *Weed Res* 29:93–96
- Burnham KP, Anderson DR (2002) Model selection and multimodel inference, 2nd edn. Springer, New York
- Carroll RJ, Ruppert D, Stefanski LA, Crainiceanu CM (2006) Measurement error in nonlinear models: a modern perspective. CRC monographs on statistics and applied probability, 2nd edn. Chapman and Hall, Boca Raton
- Cedergreen N, Ritz C, Streibig JC (2005) Improved empirical models describing hormesis. *Environ Toxicol Chem* 24:3166–3172
- Claeskens G, Hjort NL (2008) Model selection and model averaging. Cambridge University Press, Cambridge
- Darby SC, Cutter DJ, Boerma M, Constine LS, Fajardo LF, Kodama K, Mabuchi K, Marks LB, Mettler FA, Pierce LJ, Trott KR, Yeh ET, Shore RE (2010) Radiation-related heart disease: current knowledge and future prospects. *Int J Radiat Oncol Biol Phys* 76:656–665
- Darby SC, Ewertz M, McGale P, Bennet AM, Blom-Goldman U, Brønnum D, Correa C, Cutter D, Gagliardi G, Gigante B, Jensen MB, Nisbet A, Peto R, Rahimi K, Taylor C, Hall P (2013) Risk of ischemic heart disease in women after radiotherapy for breast cancer. *N Engl J Med* 368:987–998
- Ebrahimian TG, Beugnies L, Surette J, Priest N, Gueguen Y, Gloaguen C, Benderitter M, Jourdain JR, Tack K (2018) Chronic exposure to external low-dose gamma radiation induces an increase in anti-inflammatory and anti-oxidative parameters resulting in atherosclerotic plaque size reduction in ApoE<sup>-/-</sup> mice. *Radiat Res* 189:187–196
- Frey B, Hehlhans S, Rödel F, Gaipf US (2015) Modulation of inflammation by low and high doses of ionizing radiation: implications for benign and malignant diseases. *Cancer Lett* 368:230–237
- Ghobadi G, van der Veen S, Bartelds B, de Boer RA, Dickinson MG, de Jong JR, Faber H, Niemantsverdriet M, Brandenburg S, Berger RM, Langendijk JA, Coppes RP, van Luijk P (2012) Physiological interaction of heart and lung in thoracic irradiation. *Int J Radiat Oncol Biol Phys* 84(5):e639–e646
- Gillies M, Richardson DB, Cardis E, Daniels RD, O’Hagan JA, Haylock R, Laurier D, Leuraud K, Moissonnier M, Schubauer-Berigan MK, Thierry-Chef I, Kesminiene A (2017) Mortality from circulatory diseases and other non-cancer outcomes among nuclear workers in France, the United Kingdom and the United States (INWORKS). *Radiat Res* 188:276–290
- Grant EJ, Brenner A, Sugiyama H, Sakata R, Sadakane A, Utada M, Cahoon EK, Milder CM, Soda M, Cullings HM, Preston DL, Mabuchi K, Ozasa K (2017) Solid cancer incidence among the life span study of atomic bomb survivors: 1958–2009. *Radiat Res* 187:513–537
- Hoeting JA, Madigan D, Raftery AE, Volinsky CT (1999) Bayesian model averaging: a tutorial. *Stat Sci* 14:382–417
- Hoffmann S, Rage E, Laurier D, Laroche P, Guihenneuc C, Ancelet S (2017) Accounting for Berkson and classical measurement error in radon exposure using a Bayesian structural approach in the analysis of lung cancer mortality in the French Cohort of Uranium Miners. *Radiat Res* 187(2):196–209
- Hoving S, Heeneman S, Gijbels MJ, te Poele JA, Russell NS, Daemen MJ, Stewart FA (2008) Single-dose and fractionated irradiation promote initiation and progression of atherosclerosis and induce an inflammatory plaque phenotype in ApoE<sup>-/-</sup> mice. *Int J Radiat Oncol Biol Phys* 71(3):848–857
- Howe GR (1998) Use of computerized record linkage in cohort studies. *Epidemiol Rev* 20:112–121
- Howe GR, McLaughlin J (1996) Breast cancer mortality between 1950 and 1987 after exposure to fractionated moderate-dose-rate ionizing radiation in the Canadian Fluoroscopy Cohort Study and a comparison with breast cancer mortality in the Atomic Bomb Survivors Study. *Radiat Res* 145:694–707
- HPA (2010) Circulatory disease risk. Report of the Independent Advisory Group on Ionising Radiation. Health Protection Agency 2010; ISBN 978-0-85951-676-1
- ICRP (2005) Low-dose extrapolation of radiation-related cancer risk. *Ann ICRP* 35:1–140
- Kaiser JC, Walsh L (2013) Independent analysis of the radiation risk for leukaemia in children and adults with mortality data (1950–2003) of Japanese A-bomb survivors. *Radiat Environ Biophys* 52:17–27
- Kreuzer M, Auvinen A, Cardis E, Hall J, Jourdain JR, Laurier D, Little MP, Peters A, Raj K, Russell NS, Tapio S, Zhang W, Gomolka M (2015) Low-dose ionising radiation and cardiovascular diseases—strategies for molecular epidemiological studies in Europe. *Mutat Res Rev Mutat Res* 764:90–100
- Kreuzer M, Sobotzki C, Schnelzer M, Fenske N (2018) Factors modifying the radon-related lung cancer risk at low exposures and exposure rates among German uranium miners. *Radiat Res* 189:165–176
- Land CE, Kwon D, Hoffman FO, Moroz B, Drozdovitch V, Bouville A, Beck H, Luckyanov N, Weinstock RM, Simon SL (2015) Accounting for shared and unshared dosimetric uncertainties in the dose response for ultrasound-detected thyroid nodules after exposure to radioactive fallout. *Radiat Res* 183(2):159–173
- Le Gallic C, Phalente Y, Manens L, Dublineau I, Benderitter M, Gueguen Y, Lehoux S, Ebrahimian TG (2015) Chronic internal exposure to low dose <sup>137</sup>Cs induces positive impact on the stability of atherosclerotic plaques by reducing inflammation in ApoE<sup>-/-</sup> mice. *PLoS One* 10:e0128539
- Little MP (2016) Radiation and circulatory disease. *Mutat Res* 770(Pt B):299–318

- Little MP, Azizova TV, Bazyka D, Bouffler SD, Cardis E, Chekin S, Chumak VV, Cucinotta FA, de Vathaire F, Hall P, Harrison JD, Hildebrandt G, Ivanov V, Kashcheev VV, Klymenko SV, Kreuzer M, Laurent O, Ozasa K, Schneider T, Tapio S, Taylor AM, Tzoulaki I, Vandoolaeghe WL, Wakeford R, Zablotska LB, Zhang W, Lipshultz SE (2012) Systematic review and metaanalysis of circulatory disease from exposure to low-level ionizing radiation and estimates of potential population mortality risks. *Environ Health Perspect* 120:1503–1511
- Little MP, Kukush AG, Masiuk SV, Shklyar S, Carroll RJ, Lubin JH, Kwon D, Brenner AV, Tronko MD, Mabuchi K, Bogdanova TI, Hatch M, Zablotska LB, Tereshchenko VP, Ostroumova E, Bouville AC, Drozdovitch V, Chepurny MI, Kovgan LN, Simon SL, Shpak VM, Likhtarev IA (2014) Impact of uncertainties in exposure assessment on estimates of thyroid cancer risk among Ukrainian children and adolescents exposed from the Chernobyl accident. *PLoS One* 9(1):e85723
- Little MP, Kwon D, Zablotska LB, Brenner AV, Cahoon EK, Rozhko AV, Polyanskaya ON, Minenko VF, Golovanov I, Bouville A, Drozdovitch V (2015) Impact of uncertainties in exposure assessment on thyroid cancer risk among persons in Belarus exposed as children or adolescents due to the Chernobyl accident. *PLoS One* 10(10):e0139826
- Madigan D, Raftery AE (1994) Model selection and accounting for model uncertainty in graphical models using Occam's window. *J Am Statist Assoc* 89:1535–1546
- Mancuso M, Pasquali E, Braga-Tanaka I 3rd, Tanaka S, Pannicelli A, Giardullo P, Pazzaglia S, Tapio S, Atkinson MJ, Saran A (2015) Acceleration of atherosclerosis in ApoE<sup>-/-</sup> mice exposed to acute or low-dose-rate ionizing radiation. *Oncotarget* 6:31263–31271
- Mathias D, Mitchel RE, Barclay M, Wyatt H, Bugden M, Priest ND, Whitman SC, Scholz M, Hildebrandt G, Kamprad M, Glasow A (2015) Low-dose irradiation affects expression of inflammatory markers in the heart of ApoE<sup>-/-</sup> mice. *PLoS One* 10(3):e0119661
- Mitchel RE, Burchart P, Wyatt H (2007) Fractionated, low-dose-rate ionizing radiation exposure and chronic ulcerative dermatitis in normal and Trp53 heterozygous C57BL/6 mice. *Radiat Res* 168(6):716–724
- Mitchel RE, Hasu M, Bugden M, Wyatt H, Little MP, Gola A, Hildebrandt G, Priest ND, Whitman SC (2011) Low-dose radiation exposure and atherosclerosis in ApoE<sup>-/-</sup> mice. *Radiat Res* 175:665–676
- Mitchel RE, Hasu M, Bugden M, Wyatt H, Hildebrandt G, Chen YX, Priest ND, Whitman SC (2013) Low-dose radiation exposure and protection against atherosclerosis in ApoE<sup>-/-</sup> mice: the influence of P53 heterozygosity. *Radiat Res* 179:190–199
- Moseeva MB, Azizova TV, Grigoryeva ES, Haylock R (2014) Risks of circulatory diseases among Mayak PA workers with radiation doses estimated using the improved Mayak Worker Dosimetry System 2008. *Radiat Environ Biophys* 53:469–477
- NCRP (2018) Implications of recent epidemiologic studies for the linear nonthreshold model and radiation protection. Commentary No. 27. National Council on Radiation Protection and Measurements, Bethesda
- Noble RB, Bailer AJ, Park R (2009) Model-averaged benchmark concentration estimates for continuous response data arising from epidemiological studies. *Risk Anal* 29:558–564
- Ozasa K, Shimizu Y, Suyama A, Kasagi F, Soda M, Grant EJ, Sakata R, Sugiyama H, Kodama K (2012) Studies of the mortality of atomic bomb survivors, Report 14, 1950–2003: an overview of cancer and noncancer diseases. *Radiat Res* 177:229–243
- Ozasa K, Takahashi I, Grant EJ, Kodama K (2017) Cardiovascular disease among atomic bomb survivors. *Int J Radiat Biol* 93(10):1145–1150
- Rödel F, Frey B, Gaipf U, Keilholz L, Fournier C, Manda K, Schöllnberger H, Hildebrandt G, Rödel C (2012a) Modulation of inflammatory immune reactions by low-dose ionizing radiation: molecular mechanisms and clinical application. *Curr Med Chem* 19:1741–1750
- Rödel F, Frey B, Manda K, Hildebrandt G, Hehlhans S, Keilholz L, Seegenschmiedt MH, Gaipf US, Rödel C (2012b) Immunomodulatory properties and molecular effects in inflammatory diseases of low-dose X-irradiation. *Front Oncol* 2:1–9
- Schneider U, Ernst M, Hartmann M (2017) The dose-response relationship for cardiovascular disease is not necessarily linear. *Radiat Oncol* 12:74
- Schöllnberger H, Kaiser JC, Jacob P, Walsh L (2012) Dose-responses from multi-model inference for the non-cancer disease mortality of atomic bomb survivors. *Radiat Environ Biophys* 51:165–178
- Schöllnberger H, Eidemüller M, Cullings HM, Simonetto C, Neff F, Kaiser JC (2018) Dose-responses for mortality from cerebrovascular and heart diseases in atomic bomb survivors: 1950–2003. *Radiat Environ Biophys* 57(1):17–29
- Shimizu Y, Kodama K, Nishi N, Kasagi F, Suyama A, Soda M, Grant EJ, Sugiyama H, Sakata R, Moriwaki H, Hayashi M, Konda M, Shore RE (2010) Radiation exposure and circulatory disease risk: Hiroshima and Nagasaki atomic bomb survivor data, 1950–2003. *Brit Med J* 340:b5349
- Shore R, Walsh L, Azizova T, Rühm W (2017) Risk of solid cancer in low dose-rate radiation epidemiological studies and the dose-rate effectiveness factor. *Int J Radiat Biol* 93:1064–1078
- Shore RE, Beck HL, Boice JD Jr, Caffrey EA, Davis S, Grogan HA, Mettler FA Jr, Preston RJ, Till JE, Wakeford R, Walsh L, Dauer LT (2018) Implications of recent epidemiologic studies for the linear nonthreshold model and radiation protection. *J Radiol Prot* 38:1217–1233
- Shore RE, Beck HL, Boice JD Jr, Caffrey EA, Davis S, Grogan HA, Mettler FA Jr, Preston RJ, Till JE, Wakeford R, Walsh L, Dauer LT (2019) Recent epidemiologic studies and the linear no-threshold model for radiation protection—considerations regarding NCRP commentary 27. *Health Phys* 116:235–246
- Simonetto C, Azizova TV, Grigoryeva ES, Kaiser JC, Schöllnberger H, Eidemüller M (2014) Ischemic heart disease in workers at Mayak PA: latency of incidence risk after radiation exposure. *PLoS One* 9:e96309
- Simonetto C, Schöllnberger H, Azizova TV, Grigoryeva ES, Pikulina MV, Eidemüller M (2015) Cerebrovascular diseases in workers at Mayak PA: The difference in radiation risk between incidence and mortality. *PLoS One* 10:e0125904
- Stewart FA, Heeneman S, Te Poele J, Kruse J, Russell NS, Gijbels M, Daemen M (2006) Ionizing radiation accelerates the development of atherosclerotic lesions in ApoE<sup>-/-</sup> mice and predisposes to an inflammatory plaque phenotype prone to hemorrhage. *Am J Pathol* 168:649–658
- Takahashi I, Shimizu Y, Grant EJ, Cologne J, Ozasa K, Kodama K (2017) Heart disease mortality in the Life Span Study, 1950–2008. *Radiat Res* 187:319–332
- Tran V, Zablotska LB, Brenner AV, Little MP (2017) Radiation-associated circulatory disease mortality in a pooled analysis of 77,275 patients from the Massachusetts and Canadian tuberculosis fluoroscopy cohorts. *Sci Rep* 7:44147
- UNSCEAR (2000) Sources and Effects of Ionizing Radiation. United Nations Scientific Committee on the Effects of Atomic Radiation. UNSCEAR 2000 Report to the General Assembly, with scientific annexes. Volume II: Effects [http://www.unscear.org/docs/publications/2000/UNSCEAR\\_2000\\_Report\\_Vol.II.pdf](http://www.unscear.org/docs/publications/2000/UNSCEAR_2000_Report_Vol.II.pdf)
- Walsh L (2007) A short review of model selection techniques for radiation epidemiology. *Radiat Environ Biophys* 46:205–213
- Walsh L, Kaiser JC (2011) Multi-model inference of adult and childhood leukaemia excess relative risks based on the Japanese A-bomb

- survivors mortality data (1950–2000). *Radiat Environ Biophys* 50:21–35
- Williams LK, Csaki LS, Cantor RM, Reue K, Lawson GW (2012) Ulcerative dermatitis in C57BL/6 mice exhibits an oxidative stress response consistent with normal wound healing. *Comp Med* 62(3):166–171
- World Health Organization (2013) The top 10 causes of death. <http://who.int/mediacentre/factsheets/fs310/en/index.html>. Accessed 24 Nov 2014
- Yusuf S, Hawken S, Ounpuu S, Dans T, Avezum A, Lanas F, McQueen M, Budaj A, Pais P, Varigos J, Lisheng L, INTERHEART Study Investigators (2004) Effect of potentially modifiable risk factors associated with myocardial infarction in 52 countries (the INTERHEART study): case-control study. *Lancet* 364:937–952
- Zablotska LB, Little MP, Cornett RJ (2014) Potential increased risk of ischemic heart disease mortality with significant dose fractionation in the Canadian Fluoroscopy Cohort Study. *Am J Epidemiol* 179(1):120–131

**Publisher's Note** Springer Nature remains neutral with regard to jurisdictional claims in published maps and institutional affiliations.